

Rescue of the Osteopetrotic Defect in *op/op* Mice by Osteoblast-Specific Targeting of Soluble Colony-Stimulating Factor-1

S. L. ABOUD, K. WOODRUFF, C. LIU, V. SHEN, AND N. GHOSH-CHOUDHURY

Department of Pathology (S.L.A., K.W., N.G.-C.), University of Texas Health Science Center and the South Texas Veteran's Health Care System, Audie L. Murphy Division, San Antonio, Texas 78284; and Skeletch Inc. (C.L., V.S.), Bothell, Washington 98021

Soluble colony-stimulating factor-1 (sCSF-1) and membrane bound CSF-1 are synthesized by osteoblasts and stromal cells. However, the precise role of each form in osteoclastogenesis is unclear. In the *op/op* mouse, absence of osteoblast-derived CSF-1 leads to decreased osteoclasts and osteopetrosis. To determine whether sCSF-1 gene replacement can cure the osteopetrotic defect, we took advantage of the osteoblast specificity of the osteocalcin promoter to selectively express sCSF-1 in the bone of *op/op* mice. Transgenic mice harboring the human sCSF-1 cDNA under the control of the osteocalcin promoter were generated and cross-bred with heterozygous *op/wt* mice to establish *op/op* mutants expressing the transgene (*op/opT*). The *op/op* genotype and transgene expression were confirmed by PCR and Southern blot analysis, respectively. High levels of human sCSF-1 protein were selectively expressed in bone. At 2½ wk, *op/opT* mice showed normal growth and tooth eruption. Femurs removed at 5 and 14 wk were analyzed by peripheral quantitative computed tomog-

raphy and histomorphometry. The abnormal bone mineral density, cancellous bone volume, and growth plate width observed in *op/op* mice was completely reversed in *op/opT* mice by 5 wk, and this effect persisted at 14 wk, with measurements comparable with *wt/wt* mice at each time point. Correction of the skeletal abnormalities in the 5-wk-old *op/opT* mice correlated with a marked increase in the total osteoclast number, and their number per millimeter of bone surface compared with that of *op/op* mutants. Osteoclast number was maintained at 14 wk in *op/opT* mice and morphologically resembled *wt/wt* osteoclasts. These results indicate that sCSF-1 is sufficient to drive normal osteoclast development and that the osteocalcin promoter provides an efficient tool for delivery of exogenous genes to the bone. Moreover, targeting sCSF-1 to osteoblasts in the bone microenvironment may be a potentially useful therapeutic modality for treating bone disorders. (*Endocrinology* 143: 1942–1949, 2002)

MACROPHAGE COLONY-STIMULATING factor (CSF-1) is a key regulatory molecule for cells of the mononuclear phagocyte lineage, including monocytes, tissue macrophages, microglia, and osteoclasts (1). Activation of macrophages in multiple tissues has been shown to mediate, at least in part, the diverse biological effects of CSF-1 on male and female fertility, trophoblastic implantation, mammary gland development, dermal thickness, and neural function (2–5). In bone, CSF-1 stimulates the proliferation and differentiation of osteoclast progenitors and enhances osteoclast survival (6, 7). Osteoblasts and stromal cells are the main source of CSF-1 in the bone microenvironment, and these cells synthesize both the soluble form of CSF-1 (sCSF-1) and the membrane bound form (8). However, the precise biological effect of each form on osteoclastogenesis *in vivo* is unknown. sCSF-1 and membrane bound CSF-1 are derived by posttranscriptional processing of a common CSF-1 transcript, and the soluble form is rapidly secreted into the circulation as either a glycoprotein or proteoglycan, whereas the membrane bound form is expressed as an integral transmembrane glycoprotein (9–11).

The importance of CSF-1 in osteoclast development has

been demonstrated in studies using the osteopetrotic (*op/op*) mouse model. In the *op/op* mutant, a thymidine insertion in the coding sequence of the CSF-1 gene results in CSF-1 deficiency that, in turn, leads to decreased macrophage and osteoclast production (12–14). By 10 d of age, *op/op* mice develop an osteopetrotic phenotype characterized by stunted growth, absence of tooth eruption, and a domed skull. Failure of bone marrow transplantation to rescue the osteopetrotic phenotype and the inability of *op/op* osteoblasts to support osteoclast formation *in vitro* indicate that the primary defect in these mice is caused by a lack of osteoblast-derived CSF-1 (15, 16). The potential of sCSF-1 to cure the osteopetrotic defect has been controversial (17–20). Sundquist *et al.* (20) showed that restoration of physiological concentrations of circulating CSF-1 in *op/op* mice, from 1 d after birth, for 4 wk, only partially rescued the osteopetrosis, with persistent metaphyseal sclerosis possibly attributable to inadequate delivery of recombinant human CSF-1 to this site or to a lack of membrane bound CSF-1. Alternatively, the discrepancy between this and other studies may be attributable to differences in the dose or duration of CSF-1 administration. When Wiktor-Jedrzejczak *et al.* (19) administered high concentrations of recombinant human CSF-1 to 6-d-old *op/op* mice for 2 months, circulating CSF-1 was restored to normal levels, body weight was partially corrected, and osteopetrosis was resolved. However, osteopetrosis relapsed 1 month after cessation of CSF-1 therapy, and it could

Abbreviations: BMD, Bone mineral density; BV/TV, cancellous bone volume; pQCT, peripheral quantitative computed tomography; TRAP, tartrate resistant acid phosphatase; sCSF-1, soluble colony-stimulating factor-1.

not be reversed in mice treated after 7 d of age, suggesting that early and sustained postnatal CSF-1 protein expression in the bone microenvironment is required for complete remission of the osteopetrotic defect.

Osteoblasts play a key role in modulating osteoclast function via the release of cytokines and through cell-cell interaction (21, 22). Therefore, they provide a useful *in vivo* target for delivering exogenous genes that regulate osteoclastogenesis. In the present study, we took advantage of the tissue specificity of the osteocalcin promoter to selectively target sCSF-1 to osteoblasts in the bone microenvironment (23, 24). Osteocalcin is an abundant bone matrix protein expressed by mature osteoblasts but not by osteoprogenitor cells. To determine whether sCSF-1 can rescue the osteopetrotic defect, *op/op* mice carrying an osteocalcin promoter-driven human sCSF-1 transgene (*op/opT*) were generated. At 5 and 14 wk, resolution of osteopetrosis was assessed using peripheral quantitative computed tomography (pQCT) scanning, tartrate resistant acid phosphatase (TRAP) staining of osteoclasts on histologic preparations, and histomorphometric analysis.

Materials and Methods

Animals

Transgenic mice were prepared using the B6C3 strain, which is the same background as the *op/op* mouse. These mice and heterozygote mice for the *op/op* mutation (*op/wt*) were purchased from The Jackson Laboratory (Bar Harbor, ME). Animals were maintained and used according to the principals outlined in the Guide for the Care and Use of Laboratory Animals, prepared by the Institute of Laboratory Animal Resources, National Research Council.

Generation of *op/op* mice expressing sCSF-1

The transgene consists of the osteocalcin promoter linked to the sCSF-1 cDNA. The 1.8-kb 5'-flanking sequence of the rat osteocalcin promoter in sp64 (Genentech, Inc., San Francisco, CA) was digested with *SmaI-HindIII*, subcloned into the *HincII* site of pUC7, and then inserted into the *BAMHI* site of the pBSpKCR3 vector (24). The 1.8-kb CSF-1 cDNA that encodes the full-length human sCSF-1 was excised from p3ACSF-RI (Genetics Institute, Cambridge, MA) with *XhoI-EcoRI*, subcloned into the *HincII* site of pUC7 and then inserted into the *EcoRI*-digested pBSpKCR3 (obtained from Dr. Windle, University of Texas Health Science Center, San Antonio, TX) (25). In this vector, the sCSF-1 cDNA is inserted into a fragment of the rabbit β -globin gene that provides an intron and polyadenylation signal required for efficient expression of the transgene. Transgenic mice were generated, according to standard methods, at the San Antonio Cancer Institute Transgenic Facility, University of Texas Health Science Center, San Antonio (26). The *Clal-NotI*-digested fragment was microinjected into fertilized eggs derived from the mating of B6C3 mice and implanted into the oviducts of pseudopregnant CD-1 foster females. Offspring were screened for the transgene by Southern blot hybridization of tail DNA with the osteocalcin-CSF-1 injection fragment. Three founders were identified with 4–5 copies of the transgene per haploid genome. Transgenic lines were established by breeding founders to B6C3 mice. One line, showing the highest CSF-1 protein levels in bone lysates, was selected for breeding with heterozygous *op/wt* mice to generate CSF-1 transgenic *op/wt* (*op/wtT*) mice. These mice were then interbred to establish *op/op* mice expressing the transgene (*op/opT*). At 5 and 14 wk, *op/opT* mice were killed and weighed, and bone and plasma CSF-1 protein levels were determined. Age-matched *wt/wt* and *op/op* littermates served as normal and mutant controls, respectively. Femurs and tibias were excised, and a portion was frozen in liquid nitrogen for CSF-1 protein analysis. The remaining bones were fixed in 10% formalin for 2 d before pQCT, histologic, and histomorphometric analysis. Four to five femurs were analyzed at each time point, and results are expressed as mean \pm SE.

Analysis of transgene expression

Human CSF-1 protein levels were measured in plasma, bone, and tissue extracts. Two tibias were rapidly dissected and frozen in liquid nitrogen before being crushed and homogenized in TENES V buffer [50 mM Tris-HCl (pH 7.4), 1% NP-40, 2 mM EDTA, 100 mM NaCl, 10 mM sodium oxyvanadate] containing proteinase inhibitors (1 mM phenylmethylsulfonyl fluoride, 10 μ g/ml leupeptin, 20 μ g/ml aprotinin). Tissues harvested from mice were frozen and then homogenized in the same buffer. After centrifugation, bone, tissue, and plasma samples were diluted 1:2–1:6 and assayed using the human Quantikine enzyme-linked immunoassay kit (R&D Systems, Minneapolis, MN) according to the manufacturer's instructions. CSF-1 concentrations were calculated from a standard curve (31.2–2000 pg/ml) using log-log linear regression. This assay specifically detects human CSF-1 and shows negligible species cross-reactivity. The sensitivity of the test is less than 9 pg/ml.

PCR detection of *op* genotype

The *op* allele was identified using PCR to amplify the segment containing the *op* mutation on chromosome 3, as previously described (27). Genomic DNA from tails was extracted using the QIAamp Tissue Kit (QIAGEN, Chatsworth, CA). Two primers (5'-TG TGTCCCTTCCTCA-GATTACA-3' and 5'-GGTCTCATCTATTATGTCTTGTACCAGCCA-AAA-3'), designed to generate PCR products of 195 bp (*wt* allele) or 196 bp (*op* allele), were used. A 2-bp mismatch in the 3'-antisense primer (*underlined*) introduced a second *BglI* site into the PCR product spanning the extra base of the *op* mutation that was absent from the PCR product from the wild-type template. Conditions for PCR reactions were 3 min at 94 C; 1 min at 94 C, 2 min at 62 C, and 2 min at 72 C for 40 cycles; and 10 min at 72 C. Twenty microliters of PCR product was then digested with 1 μ l *BglI* for 2 h. The fragments were separated by electrophoresis in a 4% Metaphor agarose gel and visualized by ethidium bromide staining.

Bone mineral density (BMD) measurement

BMD of the femurs was measured by pQCT (RM 3000 pQCT, Norland Medical Systems, Inc., Fort Atkinson, WI). Quantitative readings were obtained at the metaphysis (12% from the distal end) and diaphysis (50% from the distal end). At each site, a 0.5-mm segment was scanned, and the BMD was calculated using small-animal software.

Histology and histomorphometric measurements

The distal half of each femur was decalcified in 10% sodium EDTA in 0.1 M phosphate buffer (pH 7.0) at 4 C for 4 d. The samples were dehydrated through standard graded alcohol solutions and embedded in glycol methacrylate using a JB-4 embedding kit (Polysciences, Inc., Warrington, PA). Tissues were sectioned longitudinally, at 4 mm, using a Jung Ultracut microtome (Reichert-Jung, Heidelberg, Germany), and the sections were stained for tartrate-resistant acid phosphatase activity followed by thionin green counterstaining (28). Static parameters were measured in a 2-mm square, 1 mm distal to the lowest point of the growth plate in the secondary spongiosa. Bone and osteoclast surfaces were traced; and cancellous bone volume (BV/TV), trabecular measurements, osteoclast numbers, and surfaces were calculated using Osteomeasure software (Osteometrics, Atlanta, GA), as we have previously described (29). The growth plate width was the average of the measurements at four equal distances along the growth plate.

Results

Generation and identification of *op/op* mice expressing the sCSF-1 transgene (*op/opT*)

Transgenic mice harboring the full-length human sCSF-1 cDNA driven by a 1.8-kb osteocalcin promoter were generated (CSF-1T). Three founders were identified; however, only one transgenic line was shown to express sCSF-1. By 14 wk of age, high human sCSF-1 levels were detected in bone extracts of these transgenic animals (1,588 pg/mg protein),

whereas plasma levels were 247 pg/ml. To further confirm tissue specificity of the transgene, CSF-1T tissue extracts were assayed for human sCSF-1 protein. Little or no sCSF-1 was detected in tissues other than bone, with results (in pg/mg protein) showing: 1.19 in brain, 1.81 in heart, not detected in lung, 4.51 in thymus, 0.69 in liver, 2.98 in spleen, 0.84 in kidney, 0.55 in gut, and 5.42 in muscle.

These CSF-1T mice were then used to generate *op/opT* mice, and the *op/op* genotype was confirmed by PCR analysis as shown in Fig. 1 (left panel). An ethidium bromide-stained 4% agarose gel of *Bgl*I-digested PCR products shows a 96-bp fragment in all cases and fragments diagnostic of either the *op* allele (70 and 30 bp) or *wt* allele (99 bp). DNA isolated from transgenic mice in lanes 1 and 2 shows the *wt/wt* genotype, whereas DNA in lanes 7 and 8 shows the *op/op* genotype. DNA from *op/wt* mice in lanes 3–6 shows the expected 99- and 96-bp fragments, along with the 70- and 30-bp fragments, which stain less intensely than those observed in *op/op* mice because of the presence of only a single *op* allele. Ten days after birth, *op/opT* mice began to show tooth eruption; and, by 2½ wk, eruption of the upper and lower incisors was comparable with *wt/wt* littermates, whereas *op/op* mice remained toothless (Fig. 1, right panel).

Analysis of CSF-1 transgene expression and body weight of *op/opT* mice

To determine the level of transgene expression in *op/opT* mice, CSF-1 protein levels were measured in bone extracts, and plasma samples were obtained from *wt/wt* and *op/opT* mice at 5 and 14 wk. High levels of human sCSF-1 protein were selectively expressed in the bone and plasma of 5-wk-old *op/opT* mice (1,570 pg/mg protein and 1,362 pg/ml, respectively). This effect persisted in bone at 14 wk; however, plasma levels declined to 315 pg/ml. At 5 wk, the weight of *op/op* mice was approximately half that of the *wt* littermates. Expression of sCSF-1 in *op/op* mice was sufficient to correct their growth rate, with the body weight of *op/opT* mice similar to that of the *wt/wt* controls at 5 and 14 wk.

Radiographic and BMD measurements in *op/opT* mice

Skeletal growth and development in *op/opT* mice were significantly improved, compared with *op/op* mice. As shown in Fig. 2, x-rays of *op/op* mice at 5 and 14 wk show marked skeletal sclerosis, with short and thickened long bones. There is dense, radiopaque bone in the iliac crest, and in the tibial and femoral metaphysis, with obliteration of marrow spaces that normally appear radiolucent. The caudal vertebrae of the tail also appear sclerotic. In contrast, *op/opT* mice show resolution of metaphyseal sclerosis by 5 wk and radiolucent marrow spaces in the iliac crest, caudal vertebrae, tibial, and femoral metaphyses comparable with *wt/wt* controls at 5 and 14 wk.

To more accurately evaluate the skeletal changes in *op/opT* mice, BMD measurements of the femurs, using pQCT, were performed. pQCT images of the metaphysis and diaphysis of femurs, isolated from *wt/wt*, *op/opT*, and *op/op* mice at 5 and 14 wk, are shown in Fig. 3A. At 5 and 14 wk, the metaphysis in *op/op* mice shows an osteopetrotic pattern characterized by lack of a clear cortical envelope and calcified cartilage in all four quadrants. The diaphysis at 5 wk shows an abundant amount of unresorbed bone with marked narrowing of the marrow cavity. By 14 wk, there is early expansion of the marrow cavity, with this region containing bone of increased density, compared with *op/opT* and *wt/wt* mice. These abnormalities were completely reversed in 5-wk-old *op/opT* mice and persisted at 14 wk, with the metaphysis showing features of normal cancellous bone and the diaphysis showing bone of normal thickness with an enlarged marrow cavity comparable with *wt/wt* mice at each time point. Quantitative analysis of BMD at each site confirms these findings, with equivalent measurements observed in 5- and 14-wk *op/opT* and *wt/wt* mice. As shown in Fig. 3B, the increased BMD in the femoral diaphysis of *op/op* mice declined to close-to-normal values of 572 mg/cm³ in *op/opT* mice by 5 wk. With age, the BMD in the femoral diaphysis increased in *op/opT* mice and was comparable with *wt* littermates. The BMD in the femoral metaphysis of *op/opT* mice was also similar to *wt/wt* mice, averaging 423 mg/cm³ at 5 wk and 545 mg/cm³

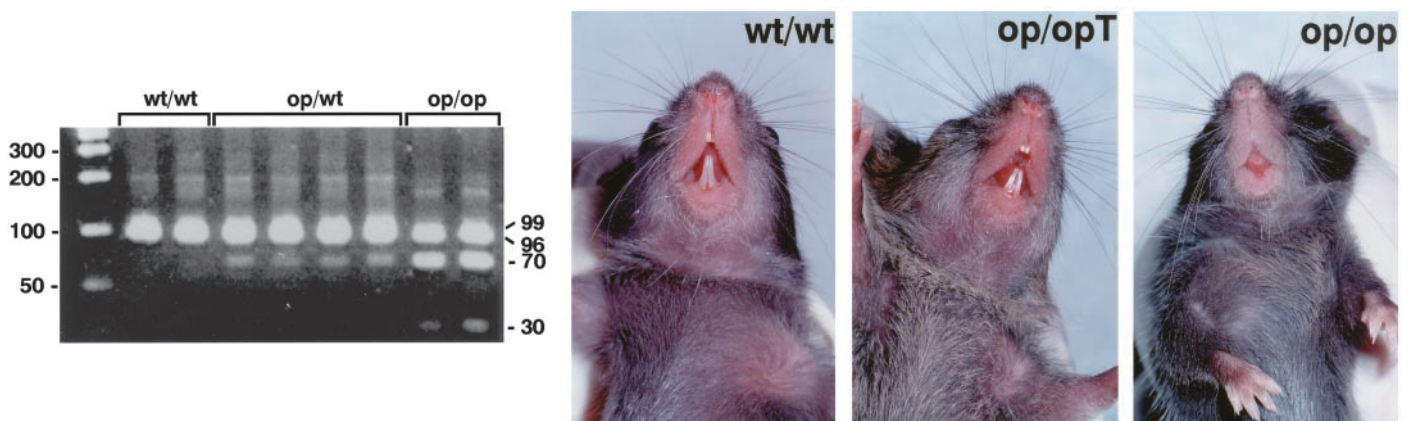


FIG. 1. Identification of the *op* genotype using PCR analysis (left panel) and correction of tooth eruption in *op/opT* mice (right panel). Ethidium bromide-stained 4% agarose gel of *Bgl*I-digested PCR products generated from *wt/wt* (lanes 1 and 2), *op/wt* (lanes 3–6), and *op/op* (lanes 7 and 8) templates shows fragments diagnostic of the *op* allele (70 and 30 bp) and *wt* allele (99 bp). At 2½ wk, *op/opT* mice show eruption of upper and lower incisors comparable with those of *wt/wt* littermates, whereas *op/op* mice are toothless.

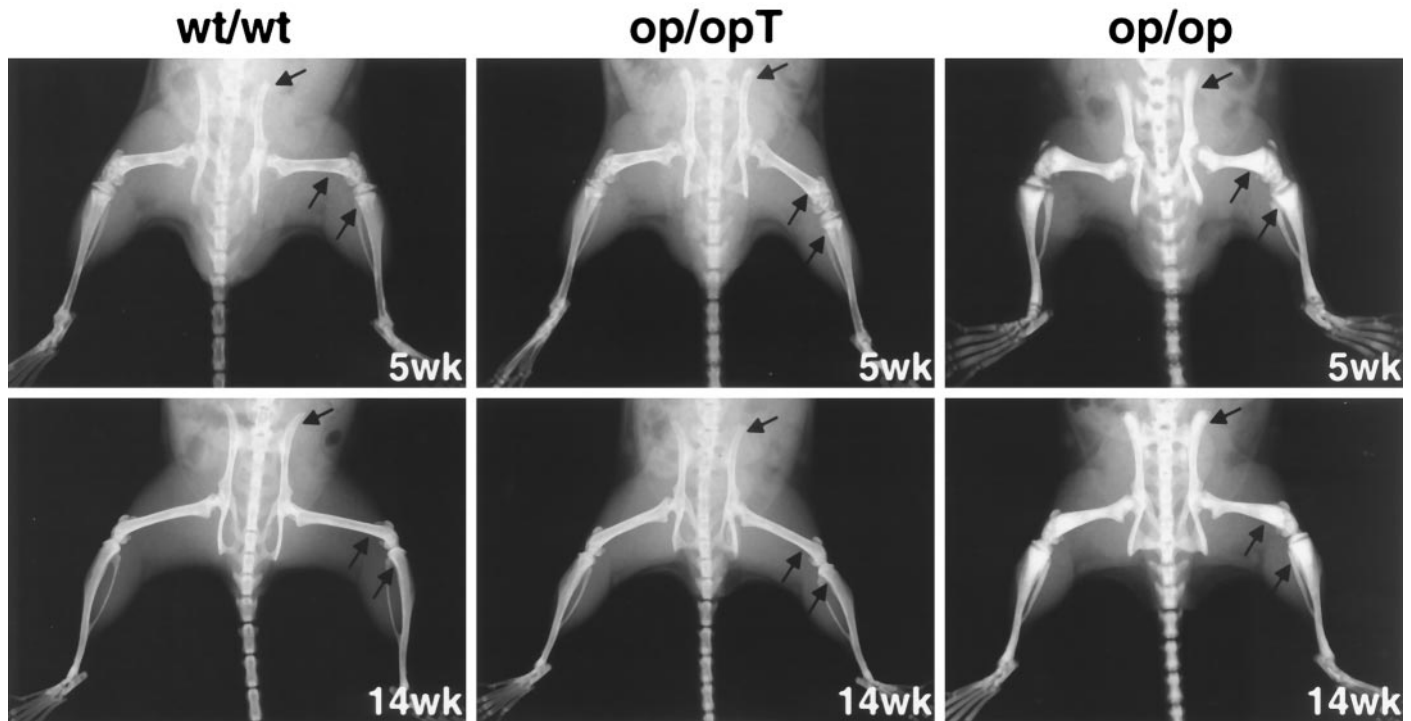


FIG. 2. Comparative radiographic findings in *wt/wt*, *op/opT*, and *op/op* mice at 5 and 14 wk. At each time point, *op/op* mutants show skeletal sclerosis with dense, radiopaque bone in the iliac crest, tibial, and femoral metaphysis (arrows) and loss of marrow spaces. In contrast, 5- and 14-wk *op/opT* mice lack metaphyseal sclerosis and show radiolucent marrow spaces comparable with *wt/wt* controls.

at 14 wk. Although the BMD in the femoral metaphysis of *op/op* mice at 5 and 14 wk (data not shown at 14 wk) seems similar to that observed in *op/opT* and *wt/wt* mice, BMD cannot be accurately determined in this site in *op/op* femurs because of the limitations of the procedure to detect the abnormal calcified cartilage. At 14 wk, BMD in the femoral diaphysis of *op/op* mice (data not shown) was also similar to that observed in *op/opT* and *wt/wt* mice. However, the relatively higher BMD in *op/op* mice was not reflected in this measurement because of the threshold value assigned for cortical bone by the analysis system.

Histologic and histomorphometric analysis of femurs in *op/opT* mice

Correction of the BMD in *op/opT* mice was visualized at the histologic level by resolution of osteopetrosis and restoration of the osteoclast population. Figure 4 shows histologic preparations of the distal femoral metaphysis from *wt/wt*, *op/opT*, and *op/op* mice. In 5- and 14-wk-old *op/op* mutants, there are thick irregular bars of calcified cartilage below the epiphyseal plate that extend into the metaphysis and replace the marrow cavity. Few TRAP-positive cells are identified in the metaphysis or along the thick cartilaginous bars. At 5 wk, *op/opT* mice are completely rescued, and this effect persisted at 14 wk, with histologic findings comparable with *wt/wt* mice at each time point. In these femurs, metaphyseal sclerosis is absent, numerous TRAP-positive osteoclasts are identified in the metaphysis and along thin bony trabeculae, and the marrow cavity is expanded with normal hematopoietic elements.

The distal femoral metaphysis of *op/opT*, compared with

wt/wt and *op/op* mice, was studied in more detail using histomorphometric analysis as shown in Table 1. The abnormal BV/TV observed in *op/op* mice was completely normalized in *op/opT* mice by 5 wk and remained comparable with *wt/wt* mice at 14 wk, with values of 17% and 23%, respectively. Similarly, the increased width of the growth plate in 5-wk-old *op/op* mice normalized in *op/opT* mice to 179 μ m by 5 wk, an effect that persisted for 14 wk. Recovery of BV/TV and growth plate width in *op/opT* mice at 5 wk correlated with a marked increase in osteoclast numbers, compared with *op/op* mutants. At 5 wk, osteoclasts were barely detectable in *op/op* mice, whereas approximately 50–55 osteoclasts were measured in both *op/opT* and *wt/wt* mice. Osteoclasts remained elevated at 14 wk and mimicked the level observed in *wt/wt* mice. Moreover, the number of osteoclasts per millimeter of bone surface in *op/opT* mice was comparable with *wt/wt* mice. Osteoclasts in *op/opT* mice were multinucleated, stained strongly with TRAP, and morphologically resembled *wt/wt* osteoclasts, whereas those in *op/op* mice tended to be mononucleated and weakly positive for TRAP staining. Other histomorphometric parameters were also corrected in *op/opT* mice, including trabecular thickness, number and separation, total length of osteoclast surface, and percent bone surface covered by osteoclasts (osteoclast surface/BS); and results were not significantly different between *op/opT* and *wt/wt* groups.

Discussion

Results from this study indicate that osteoblast-targeted sCSF-1 gene expression is sufficient to drive normal osteoclast development. In *op/opT* mice, the osteocalcin promoter

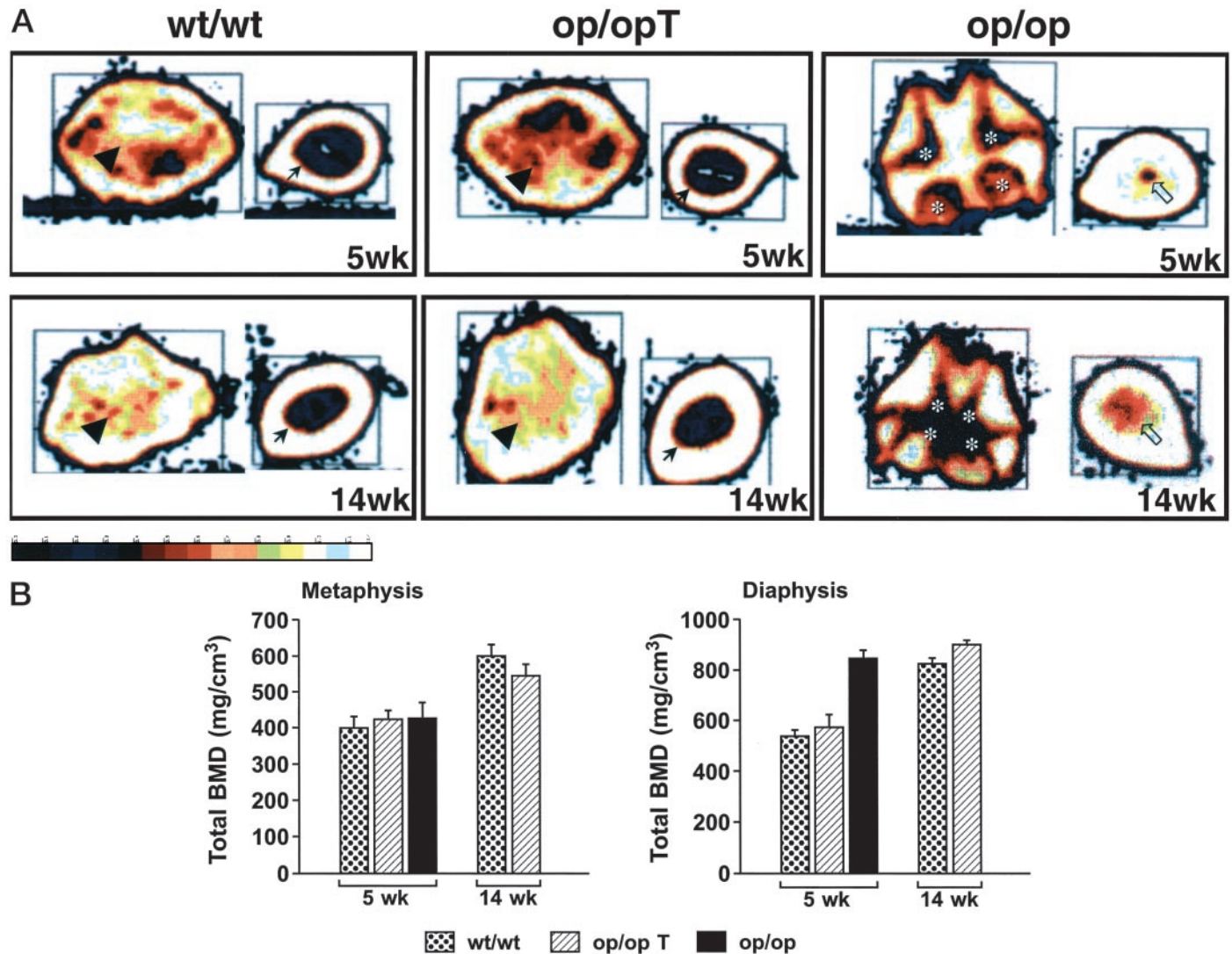


FIG. 3. Comparative BMD measurements in *wt/wt*, *op/opT*, and *op/op* mice at 5 and 14 wk. A, pQCT images of femurs were obtained at the metaphysis (left side of each panel) and diaphysis (right side of each panel). The color bars indicate increasing BMD as the color intensity declines. In 5- and 14-wk *op/op* mutants, the metaphysis shows an osteopetrotic pattern with lack of a clear cortical envelope and calcified cartilage in four quadrants (asterisk). The diaphysis shows increased unresorbed bone with marked narrowing of the marrow space at 5 wk and early expansion of the marrow cavity, visualized as an enlarged area of intermediate bone density, by 14 wk (open arrows). In contrast, BMD in *op/opT* mice was similar to that in *wt/wt* mice at each time point, with the metaphysis showing normal cancellous bone (arrowheads) and the diaphysis showing bone of normal thickness with a patent marrow cavity (arrows). B, Quantitative analysis of BMD at each site in 5- and 14-wk-old *wt/wt*, *op/opT*, and *op/op* mice ($n = 5$ mice/group). Data are expressed as mean \pm SE.

showed efficient transcriptional activity, with high levels of sCSF-1 detected in bone for at least 14 wk. This prevented the development of osteopetrosis and maintained a remarkably normal skeletal phenotype in adult *op/op* mice. These findings suggest that restoration of tissue and circulating levels of CSF-1 is an efficient method for regulating osteoclastogenesis. Moreover, the osteocalcin promoter provides a useful tool for delivery of CSF-1 and other cytokines to osteoblasts that, in turn, release these factors in a physiologically appropriate manner.

Analysis of CSF-1T mice before cross-breeding confirmed selective targeting of the transgene to the bone, with little or no expression of human sCSF-1 in other tissues. Circulating levels of human sCSF-1 protein were also detectable. CSF-1T mice were established on the same genetic background as

op/op mice, to minimize any effect of strain variation on transgene expression. Similar levels of human sCSF-1 in bone of CSF-1T mice used for cross-breeding and in *op/opT* mice indicated that the transgene was efficiently transferred to *op/op* mice. Because *op/wtT* mice were interbred to generate *op/opT* mice, some mice would be expected to be homozygous or heterozygous for the transgene. The levels of transgene expression and resolution of the osteopetrotic defect in *op/opT* mice were remarkably similar among the animals examined. Successful targeting of sCSF-1 to bone in *op/opT* mice was evident by 2½ wk, when eruption of upper and lower incisors was comparable with *wt/wt* littermates. At 5 wk, high levels of sCSF were detected in bone extracts of *op/opT* but not *wt/wt* controls. Human sCSF-1 levels in bone remained elevated at 14 wk, whereas plasma levels declined.

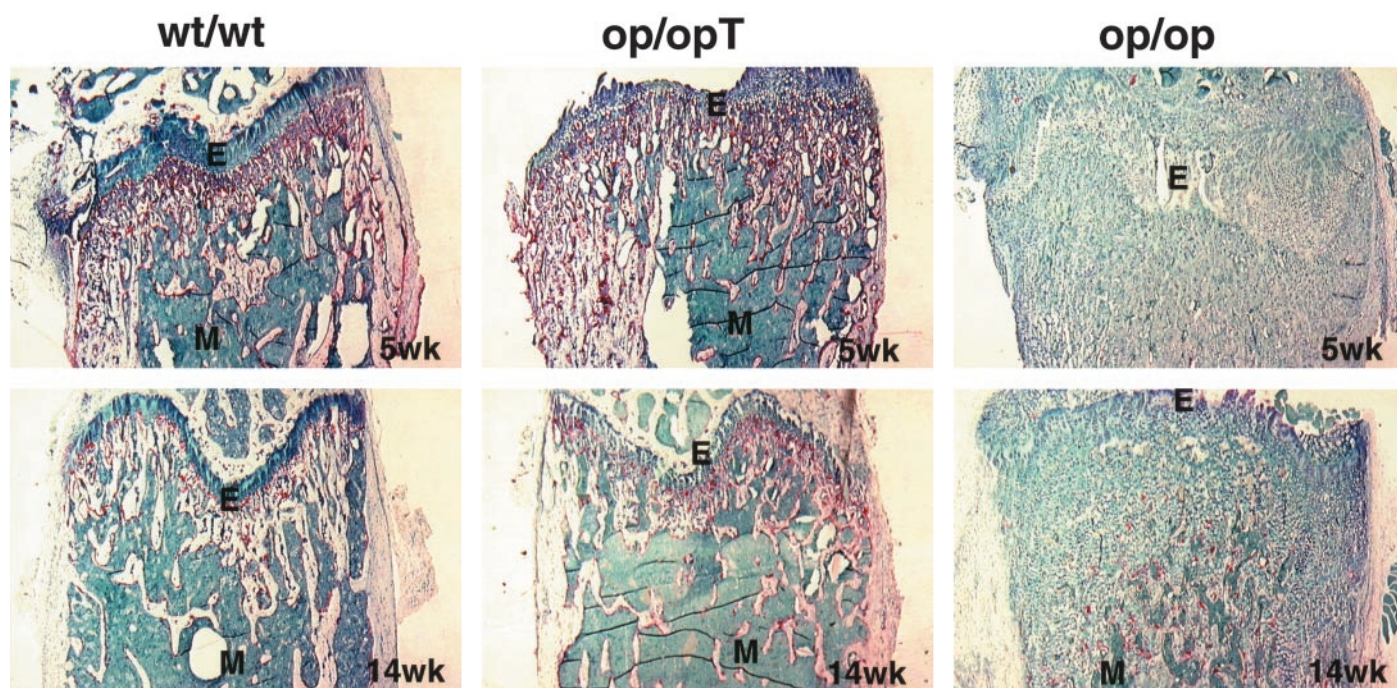


FIG. 4. Comparative histological analysis of the distal femoral metaphysis from *wt/wt*, *op/opT*, and *op/op* mice. Decalcified, plastic-embedded tissue was sectioned in the midsagittal plane and stained for TRAP activity, followed by thionin green counterstaining. The epiphyseal plate (E) and metaphysis are shown at the top of each field. In 5- and 14-wk-old *op/op* mutants, thick, irregular bars of calcified cartilage extend from the epiphyseal plate into the marrow cavity (M), with few TRAP-positive cells identified. By 5 wk, *op/opT* mice are completely rescued, and this effect persisted at 14 wk (400 \times magnification).

TABLE 1. Histomorphometric measurements

	BV/TV (%)	Growth plate width (mm)	OC no.	Trabecular thickness (μ m)	Trabecular no./mm	Trabecular separation (μ m)	OC no./mm BS	OC surface (mm)	OC surface/mm BS (%)
<i>wt/wt</i> : 5 wk	17.4 \pm 5	174 \pm 18	50.0 \pm 5	36.8 \pm 2.2	4.6 \pm 0.4	184 \pm 20.1	6.3 \pm .65	1.3 \pm 0.05	16.8 \pm 0.9
14 wk	22.9 \pm 3.5	119 \pm 8	30.0 \pm 10	45.9 \pm 2.7	5.0 \pm 0.3	156 \pm 11.6	3.5 \pm 1.3	0.69 \pm 0.11	8.2 \pm 1.4
<i>op/opT</i> : 5 wk	17.0 \pm 3	179 \pm 39	55.5 \pm 6	31.6 \pm 2.4	4.7 \pm 0.6	199 \pm 34.0	7.2 \pm 1.0	1.42 \pm 0.13	21.1 \pm 3.0
14 wk	23.0 \pm 4.4	109 \pm 6	35.0 \pm 11	43.2 \pm 2.8	5.4 \pm 0.3	145 \pm 11.6	3.8 \pm 1.5	0.77 \pm 0.12	9.2 \pm 1.6
<i>op/op</i> : 5 wk	0	420 \pm 110	2.5 \pm 3.5	NT	NT	NT	NT	NT	NT
14 wk	0	364 \pm 62	16.0 \pm 10	NT	NT	NT	NT	NT	NT

Comparative histomorphometric analysis of the distal femoral metaphysis from *wt/wt*, *op/opT*, and *op/op* mice at 5 and 14 wk. The abnormal BV/TV and growth plate width in *op/op* mice was reversed in *op/opT* mice by 5 wk and persisted at 14 wk, with measurements comparable with *wt/wt* mice at each time point (the percent BV/TV in *op/op* mice is 0, because of the absence of normal cancellous bone). This correlated with a marked increase in osteoclast numbers and their number per millimeter of bone surface in *op/opT* mice. Parameters not tested (NT) in *op/op* mice cannot be calculated because of the absence of cancellous bone (n = 4–5 mice/group). Data are expressed as mean \pm SE. OC, Osteoclast.

This decrease may have resulted from enhanced CSF-1 receptor-mediated internalization and intracellular metabolism (30). Adequate transgene expression in *op/op* mice was manifested by normalization of growth and body weight. Tooth eruption in *op/opT* mice occurred at 2½ wk, earlier than would be expected if it were attributable to spontaneous resolution (5 wk).

The radiographic changes in *op/opT* mice were dramatic, compared with *op/op* mice at 5 wk, with complete loss of metaphyseal sclerosis and radiolucent marrow spaces throughout the axial skeleton. pQCT images of femurs from 5- and 14-wk-old *op/opT* mice confirmed the presence of normal cancellous bone in the metaphysis and bone of normal thickness in the diaphysis, with an expanded marrow cavity comparable with *wt/wt* mice. These results corre-

lated with histologic analysis of *op/opT* femurs that showed normalization of the growth plate width, numerous TRAP-positive osteoclasts along thin bony trabeculae in the metaphysis, and a well-developed marrow cavity. Histomorphometric analysis confirmed that the abnormal BV/TV and growth plate width observed in *op/op* mice was completely reversed in *op/opT* mice by 5 wk and persisted at 14 wk. These findings, to our knowledge, provide the most detailed analysis of the effect of sCSF-1 on *op/op* skeletal tissues. The lack of excessive osteoclastogenesis and osteoporosis, despite the high levels of sCSF-1, is intriguing and suggests that sCSF-1 is required for restoration of normal osteoclastogenesis but may not be a critical factor that results in excessive osteoclastogenesis and bone resorption.

Under normal physiological conditions, local production

of CSF-1 by osteoblasts and their cell-to-cell interaction with osteoclast progenitors are critical for osteoclast development (21, 22, 31). Systemically administered sCSF-1 may have numerous effects on multiple organs, and it is unclear from previous studies whether the effect of sCSF-1 on bone is direct or mediated indirectly via the release of other growth factors. Our findings support a direct effect of sCSF-1 on osteoclastogenesis, with a sustained cure achieved by restoring sCSF-1 levels in the osteoblasts of *op/op* mice throughout murine development. To date, relapse of osteopetrosis has not been observed in *op/opT* mice up to 1 yr. The remarkable concordance between the *op/opT* and wild-type animals is intriguing. Our previous *in vitro* data predicted that sCSF-1 would only partially cure osteopetrosis. In coculture experiments, retrovirally transduced *op/op* stromal cells producing normal levels of sCSF-1 protein supported fewer numbers of osteoclasts, compared with normal stroma (32). However, *in vitro* studies may not mimic *in vivo* physiological conditions. It is likely that selective expression of sCSF-1 in *op/op* osteoblasts, rather than in whole-bone marrow stroma, during development provided a more physiologic milieu and restored osteoclastogenesis and corrected the skeletal abnormalities.

Similar to that in rodents, osteopetrosis in humans is a heterogeneous group of skeletal disorders characterized by reduced bone resorption caused by inactive osteoclasts (33). Although a few studies have identified mutations in the gene encoding the vacuolar proton pump as a cause of certain forms of osteopetrosis, the genetic defect(s) underlying most cases of osteopetrosis remains to be determined (34, 35). Rescue of *op/op* mice with sCSF-1 raises the possibility that a similar CSF-1-deficiency disease may also exist among the heterogeneous forms of human osteopetrosis. The use of promoters with tissue specificity has potential therapeutic application in bone disorders (36, 37). The rat osteocalcin promoter has been shown to direct osteoblast-specific expression of GH and TGF- β 2 in transgenic mice (23, 24). It has also been used for *in vivo* targeting to metastatic pulmonary osteosarcoma (38). Administration *iv* of an adenoviral vector containing an osteocalcin-thymidine kinase construct was shown to localize to tumor cells and inhibit their growth when mice were treated with ancylovir. More recently, mice transplanted with bone marrow-derived adherent cells containing the osteocalcin promoter showed reporter gene expression in the engrafted osteoblast cells (39). This suggests that exogenous genes could be delivered to the bone using *ex vivo* techniques, whereby autologous bone marrow adherent cells are expanded in culture, transduced with an osteocalcin-containing vector, and infused into the recipient. Alternatively, mature osteoblasts in the bone could be directly targeted *in vivo* using adenoviral-based gene therapy. Thus, targeting sCSF-1 or other exogenous genes to osteoblasts may provide a useful therapeutic approach for regulating osteoclast development and function in a variety of bone disorders, including osteopetrosis, osteoporosis, and bone metastasis.

Acknowledgments

We thank Dr. Christi A. Walter for help with generating transgenic mice and for valuable discussions.

Received August 30, 2001. Accepted January 15, 2002.

Address all correspondence and requests for reprints to: Sherry L. Abboud, M.D., Department of Pathology, University of Texas Health Science Center, 7703 Floyd Curl Drive, San Antonio, Texas 78284. E-mail: abbouds@uthscsa.edu.

Portions of this work were published, in abstract form, at the annual meeting of The American Society of Bone and Mineral Research, Toronto, Canada, September 22–26, 2000.

This work was supported, in part, by funding from the NIH (AR-42306, to S.L.A.), Veteran's Administration Merit Award (to S.L.A.), and Department of Defense (DAMD17-99-1-9400, to N.G.-C).

References

- Roth P, Stanley E 1992 The biology of CSF-1 and its receptor. *Curr Top Microbiol Immunol* 181:141–167
- Araki M, Fukumatsu Y, Katabuchi H, Schultz LD, Takahashi K, Okamura H 1996 Follicular development and ovulation in macrophage colony-stimulating factor-deficient mice homozygous for the osteopetrosis (*op*) mutation. *Biol Reprod* 54:478–484
- Cohen PE, Chisholm O, Arceci RJ, Stanley ER, Pollard JW 1996 Absence of colony-stimulating factor-1 in osteopetrotic (*csfm^{OP}/csfm^{OP}*) mice results in male fertility defects. *Biol Reprod* 55:310–317
- Pollard JW, Henninghausen L 1994 Colony stimulating factor-1 is required for mammary gland development during pregnancy. *Proc Natl Acad Sci USA* 91:9312–9316
- Pollard JW, Stanley ER 1996 Pleiotropic roles for CSF-1 in development defined by the mouse mutation osteopetrotic (*op*). *Adv Dev Biochem* 4:153–193
- Tanaka S, Takahashi N, Udagawa N, Tamura T, Akatsu T, Stanley ER, Kurokawa T, Suda T 1993 Macrophage colony-stimulating factor is indispensable for both proliferation and differentiation of osteoclast progenitors. *J Clin Invest* 91:257–263
- Fuller K, Owens JM, Jagger CJ, Wilson A, Moss R, Chambers TJ 1993 Macrophage colony-stimulating factor stimulates survival and chemotactic behavior in isolated osteoclasts. *J Exp Med* 178:1733–1744
- Felix R, Halasy-Nagy J, Wetterwald A, Cecchini MG, Fleisch H, Hofstetter W 1996 Synthesis of membrane- and matrix-bound colony-stimulating factor-1 by cultured osteoblasts. *J Cell Physiol* 166:311–322
- Ladner MB, Martin GA, Noble JA, Nikoloff DM, Tal R, Kawasaki ES, White TJ 1987 Human CSF-1: gene structure and alternative splicing of mRNA precursors. *EMBO J* 6:2693–2698
- Rettenmier CW, Roussel MF 1988 Differential processing of colony-stimulating factor 1 precursors encoded by two human cDNAs. *Mol Cell Biol* 8:5026–5034
- Price LKH, Choi HU, Rosenberg L, Stanley ER 1992 The predominant form of secreted colony stimulating factor-1 is a proteoglycan. *J Biol Chem* 267:2190–2199
- Yoshida H, Hayashi S-I, Kunisada T, Ogawa M, Nishikawa S, Okamura H, Sudo T, Shultz LD, Nishikawa S-I 1990 The murine mutation osteopetrosis is in the coding region of the macrophage colony-stimulating factor gene. *Nature* 345:442–444
- Wiktor-Jedrzejczak W, Bartocci A, Ferrante AW, Ahmend-Ansari A, Sell KW, Pollard JW, Stanley ER 1990 Total absence of colony-stimulating factor 1 in the macrophage-deficient osteopetrotic (*op/op*) mouse. *Proc Natl Acad Sci USA* 87:4828–4832
- Felix R, Cecchini MG, Hofstetter W, Elford PR, Stutzer A, Fleisch H 1990 Impairment of macrophage colony-stimulating factor production and lack of resident bone marrow macrophages in the osteopetrotic (*op/op*) mouse. *J Bone Miner Res* 5:781–789
- Marks Jr SC, Seifert MF, McGuire JL 1984 Congenitally osteopetrotic mice are not cured by transplants of spleen or bone marrow from normal littermates. *Metab Bone Dis Relat Res* 5:183–186
- Takahashi N, Udagawa N, Akatsu T, Tanaka H, Isogai Y, Suda T 1991 Deficiency of osteoclasts in osteopetrotic mice is due to a defect in the local microenvironment provided by osteoblastic cells. *Endocrinology* 128:1792–1796
- Felix R, Cecchini MG, Fleisch H 1990 Macrophage colony stimulating factor restores *in vivo* bone resorption in the *op/op* osteopetrotic mouse. *Endocrinology* 127:2592–2594
- Kodama H, Yamasaki A, Nose M, Niida S, Ohgame Y, Abe M, Kumegawa M, Suda T 1991 Congenital osteoclast deficiency in osteopetrotic (*op/op*) mice is cured by injections of macrophage colony-stimulating factor. *J Exp Med* 173:269–272
- Wiktor-Jedrzejczak W, Urbanowska E, Aukerman SL, Pollard JW, Stanley ER, Ralph P, Ansari AA, Sell KW, Szperl M 1991 Correction by CSF-1 of defects in the osteopetrotic *op/op* mouse suggests local, developmental, and humoral requirements for this growth factor. *Exp Hematol* 19:1049–1054
- Sundquist KT, Cecchini MG, Marks Jr SC 1995 Colony-stimulating factor-1 injections improve but do not cure skeletal sclerosis in osteopetrotic (*op*) mice. *Bone* 16:39–46

21. Kodama H, Nose M, Niida S, Yamasaki A 1991 Essential role of macrophage colony-stimulating factor in the osteoclast differentiation supported by stromal cells. *J Exp Med* 173:1291–1294
22. Takahashi N, Akatsu T, Udagawa N, Sasaki T, Yamaguchi A, Moseley JM, Martin TJ, Suda T 1998 Osteoblastic cells are involved in osteoclast formation. *Endocrinology* 123:2600–2602
23. Baker AR, Hollingshead PG, Pitts-Meek S, Hansen S, Taylor R, Stewart TA 1992 Osteoblast-specific expression of growth hormone stimulates bone growth in transgenic mice. *Mol Cell Biol* 12:5541–5547
24. Erlebacher A, Derynck R 1996 Increased expression of TGF-beta2 in osteoblasts results in osteoporosis-like phenotype. *J Cell Biol* 132:195–210
25. Wong GG, Temple PA, Leary AC, Witek-Giannotti JS, Yang YC, Ciarletta AB, Chung M, Murtha P, Kriz R, Kaufman RJ 1987 Human CSF-1: molecular cloning and expression of a 4 kb cDNA encoding the human urinary protein. *Science* 235:1504–1508
26. Sigmund CD 1993 Major approaches for generating and analyzing transgenic mice. *Hypertension* 22:599–607
27. Lieschke GJ, Stanley E, Grail D, Hodgson G, Sinickas V, Gall JA, Sinclair RA, Dunn AR 1994 Mice lacking both macrophage- and granulocyte-macrophage colony stimulating factor have macrophages and coexistent osteopetrosis and severe lung disease. *Blood* 84:27–35
28. Liu CC, Sanghri R, Burnell JM, Howard GA 1987 Simultaneous demonstration of bone alkaline and acid phosphatase activities in plastic-embedded sections and differential inhibition of the activities. *Histochemistry* 86:559–566
29. Meng XW, Liang XG, Birchman R, Wu DD, Demspter DW, Lindsay R, Shen V 1996 Temporal expression of the anabolic action of PTH in cancellous bone of ovariectomized rats. *J Bone Miner Res* 11:421–429
30. Bartocci A, Mastrogiannis DS, Migliorati G, Stockert RJ, Wolkoff AW, Stanley ER 1987 Macrophages specifically regulate the concentration of their own growth factor in the circulation. *Proc Natl Acad Sci USA* 84:6179–6183
31. Felix R, Hofstetter W, Wetterwald A, Cecchini MG, Fleisch H 1994 Role of colony stimulating factor-1 in bone metabolism. *J Cell Biochem* 55:340–349
32. Abboud SL, Woodruff KA, Ghosh-Choudhury G 1998 Retroviral-mediated gene transfer of CSF-1 into *op/op* stromal cells to correct defective *in vitro* osteoclastogenesis. *J Cell Physiol* 176:323–331
33. Fasth A, Porras O 1999 Human malignant osteopetrosis: pathophysiology, management and the role of bone marrow transplantation. *Pediatr Transplant* 3 (Suppl 1):102–107
34. Kornak U, Schulz A, Friedrich W, Uhlhass S, Kremens B, Voit T, Hasan C, Bode U, Jentsch TJ, Kubisch C 2000 Mutations in the $\alpha 3$ subunit of the vacuolar H(+)-ATPase cause infantile malignant osteopetrosis. *Hum Mol Genet* 9:2059–2063
35. Frattini A, Orchard PJ, Sobacchi C, Giliani S, Abinun M, Mattsson JP, Kelling DJ, Andersson AK, Wallbrandt P, Zecca L, Notarangelo LD, Vezzoni P, Villa A 2000 Defects in TCIRG1 subunit of the vacuolar proton pump are responsible for a subset of human autosomal recessive osteopetrosis. *Nat Genet* 25:343–346
36. Vile RG, Nelson JA, Castleden S, Chong H, Hart IR 1994 Systemic gene therapy of murine melanoma using tissue specific expression of the HSVtk gene involves an immune component. *Cancer Res* 54:6228–6234
37. Sokol DL, Gerwitz AM 1996 Gene therapy: basic concepts and recent advances. *Crit Rev Eukaryot Gene Expr* 6:29–57
38. Shirakawa T, Ko SC, Gardner TA, Cheon J, Miyamoto T, Gotoh A, Chung LW, Kao C 1998 *In vivo* suppression of osteosarcoma pulmonary metastasis with intravenous osteocalcin promoter-based toxic gene therapy. *Cancer Gene Ther* 5:274–280
39. Hou Z, Nguyen Q, Frenkel B, Nilsson SK, Milne M, van Wijnen AJ, Stein JL, Quesenberry P, Lian JB, Stein GS 1999 Osteoblast-specific gene expression after transplantation of marrow cells: implications for skeletal gene therapy. *Proc Natl Acad Sci USA* 96:7294–7299